Cocrystallization in Piperazine-Based Polyamide Copolymers: Small- and Wide-Angle X-ray Diffraction Studies at 30 °C

Sven Hoffmann,[†] Bert Vanhaecht,[‡] Jan Devroede,[‡] Wim Bras,[†] Cor E. Koning,[‡,§] and Sanjay Rastogi*,[⊥]

Netherlands Organisation of Scientific Research NWO, Dutch Belgian Beamline, European Synchrotron Radiation Facility, B. P. 220, 38043 Grenoble, France; Department of Physical and Colloidal Chemistry, Free University of Brussels, Pleinlaan 2, 1050 Brussels, Belgium; and Laboratory of Polymer Technology and Laboratory of Polymer Chemistry, Eindhoven University of Technology TUE, P.O. Box 513, 5600 MB Eindhoven, The Netherlands

Received July 27, 2004; Revised Manuscript Received December 22, 2004

ABSTRACT: Copolyamides, based on 1,12-dodecanedicarboxylic acid and different ratios of 1,2-ethylenediamine and piperazine, i.e., PA-(2.14-*co*-pip.14), as well as the corresponding homopolymers PA-2.14 and PA-pip.14, were studied by SAXS and WAXS. Up to a pip mole ratio of 0.62, the 2.14 and pip.14 units cocrystallize in a common crystal lattice, slightly deviating from the structure of homopolyamide 2.14. The hydrogen bonds obviously tolerate significant amounts of comonomer before the crystal structure is changed significantly. For pip mole percentages of 0.90 and higher, both repeating units cocrystallize in a slightly distorted PA-pip.14 crystal structure. For pip mole percentages of 0.70 and 0.82, however, the X-ray patterns show peaks that stem from both the PA-2.14- and the PA-pip.14-like crystalline structure, indicating that the two structures coexist in this composition range. Since the intersheet distance practically remains unaffected upon incorporation of the piperazine rings, it is concluded that these rings are oriented parallel to the hydrogen-bonded sheets. Furthermore, from the composition dependency of the experimentally determined lattice spacings, keeping in mind that the intersheet distance is constant, it is concluded that the hydrogen-bonded sheets are shifted parallel to one another.

Introduction

The advantageous properties of polyamides like the high melting point and material strength are well-known. The number of inter- and intramolecular hydrogen bonds in polyamides is intimately linked to their material properties, and by varying the hydrogen bond density, these material properties can be influenced to a large degree. One possible approach to control the hydrogen bond density, and therewith thermal transitions and other physical properties, is to modify the length of the aliphatic portions of linear polyamide chains.[1−3] In this way, the spatial separation between the amide groups, responsible for the hydrogen bond formation, is easily altered, and consequently the overall density of hydrogen bonds in the system can be adjusted. An alternative strategy to vary the hydrogen bond density is to replace the amide group by a different chemical unit that reduces the possibility to form hydrogen bonds but provides similar structural features.

In this study, we report on the effects of replacing a varying fraction of 1,2-ethylenediamine (1,2-EDA) residues of conventional polyamide-2.14 (PA-2.14) by piperazine groups.[4] The chemical structures of the two corresponding amide units are shown in Figure 1. In contrast to 1,2-EDA-based monomer residues, the piperazine-based residues do not contain any amide hydrogens and thus are not able to act as hydrogen bond donors. Nevertheless, they still can serve as acceptors for hydrogen bonds due to the unchanged number of carbonyl groups in the molecules. When the polymer is made exclusively of piperazine-based repeating units, a homopolymer, entirely free of hydrogen bonds, is obtained and is referred to as polyamide-pip.14 (PA-pip.14) in this work. Investigations based on thermal analysis, solid-state NMR, and results from wide-angle X-ray scattering (WAXS) have shown that 1,2-EDA- and piperazine-based polyamide units can cocrystallize into a single-crystalline structure. This is true for both binary blends of the two homopolymers PA-2.14 and PA-pip.14 as well as for copolymers PA-(2.14-*co*-pip.14), which contain both types of chemical building units.[4]

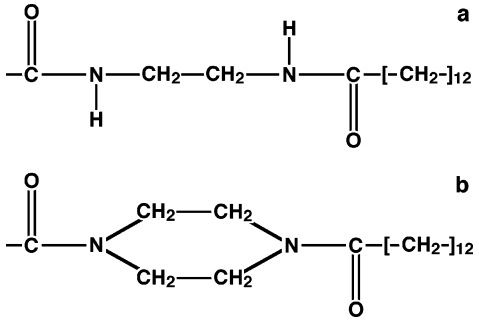

Figure 1. Chemical structure of (a) 1,2-EDA- and (b) piperazine-based repeating units.

The typical crystalline structure of most common polyamide systems consists of a succession of flat, hydrogen-bonded sheets, in which the polyamide molecules are arranged in a parallel way.[5] In PA-2.14, these sheets, held together by relatively weak van der Waals forces, are stacked with a progressive lateral translation from one plane to the next.[6,7] The same structure is found in the case of many other even−even polyamides,[8−11] where even−even stands for an even number of backbone carbon atoms in the diamine as well as in the

* Author for correspondence.
[†] NWO.
[‡] Free University of Brussels.
[§] TUE, Polymer Chemistry.
[⊥] TUE, Polymer Technology.

10.1021/ma048456e CCC: $30.25
Published on Web 02/09/2005

dicarboxylic acid residue. The unit cell of the crystallites is triclinic and is described by a set of six lattice parameters: the length of the three lattice vectors (**a**, **b**, **c**) and the three angles they enclose (α, β, γ).

For polyamides, the diffracted X-ray intensity is in general dominated by four strong reflections that are indexed as 001, 010, 100, and 110, where the lattice spacing corresponding to the 010 and the 110 reflections are nearly identical.[5] Therefore, the two reflections 010 and 110 cannot be separated in experimental WAXS patterns taken on isotropic samples. For the family of 2.2n-type polyamides (n: integer number), the 100 and 010/110 reflections are found at a scattering vector of amplitude $Q = 1.52$ and 1.62 Å^{-1} ($Q = (4\pi/\lambda) \sin \vartheta$, λ = wavelength of incident radiation, 2ϑ = scattering angle), respectively, and depend only weakly on the value of the index n.[6,7] The position of the 001 reflection, on the other hand, is more or less proportional to $1/n$ because the repeat distance of the crystalline structure in the direction of the c axis is proportional to the length of a monomer unit of the polymer. An interpolation of results by Jones et al.[6] and Li and Yan[7] on different 2.2n polyamides results in a value of $Q_{001} = 0.326$ Å^{-1} for PA-2.14.

Here, we present results from studies utilizing different X-ray diffraction techniques in order to achieve more detailed information on how the piperazine-based polyamide units are built into the crystalline structure of PA-2.14 and which modifications to the crystalline structure this entails. To this purpose, we focus on structural features of recrystallized PA-(2.14-*co*-pip.14) copolymers as a function of the molar fraction of piperazine-based repeating units.

Experimental Section

a. Materials. The homopolymers PA-2.14 and PA-pip.14, as well as copolymers PA-(2.14-*co*-pip.14) with different piperazine fractions, were synthesized via a solution polycondensation reaction of 1,12-dodecanedicarbonyl dichloride and different amounts of 1,2-EDA and piperazine. The composition of the resulting copolyamides was determined by solution ^{13}C NMR spectroscopy. The synthesis and characterization of the polyamide materials used in the this study have been described elsewhere.[4] Piperazine-based copolyamides with a molar fraction of $x_{pip} = 0.28$, 0.30, 0.46, 0.54, 0.62, 0.70, 0.82, and 0.90 (all ±3%) have been used in the experiments reported here. These copolymers will be referred to as coPA 0.28 to 0.90.

b. Methods. All samples were prepared by a heating and cooling cycle, starting near room temperature with as-synthesized samples and reaching temperatures well above the respective melting points. Constant heating and cooling rates of 10 K/min were used. After this preparative heat treatment, X-ray diffraction measurements were performed at a sample temperature of 30 °C on materials that can be considered to have a comparable and well-defined thermal history. Three instrumental devices were employed covering the different structural and morphological features in the scattered X-ray intensity: the X-ray powder diffractometer (XPD) of the ID11 beamline using a plate transmission setup with a position-sensitive detector,[12] the SAXS/WAXS station of BM26B,[13] and the SAXS/WAXS setup of ID2,[14] all situated at the European Synchrotron Radiation Facility, Grenoble, France. ID11 was used to cover the three main crystalline reflections of the two homopolyamides PA-2.14 and PA-pip.14 and of the copolyamides with $x_{pip} = 0.28$, 0.46, and 0.54 by SAXS on BM26B and the 100 and 010/110 reflections simultaneously by WAXS. The X-ray scattering from the stacking of the crystalline lamellae was measured by SAXS for PA-2.14, PA-pip.14, and coPA 0.30, 0.46, 0.82, and 0.90. SAXS and WAXS patterns for all copolyamides and the two homopolymers were collected on ID2 and cover all three crystalline reflections as well as the signal corresponding to the lamellar stacks of crystallites. The diffraction patterns were taken immediately after the heating−cooling cycle in the case of the ID11 and BM26B measurements. The ID2 measurements were carried out several hours after the preparative heat treatment. Hereby, the crystalline structure was purposely allowed to relax at room temperature during this annealing time prior to the X-ray scattering measurements.

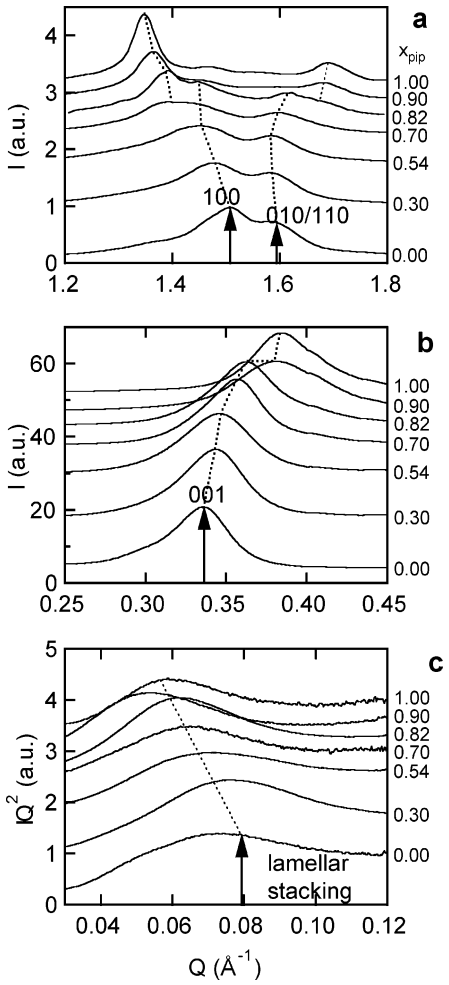

Figure 2. Examples for the X-ray diffraction from the SAXS/WAXS station of ID2 on copolyamides with the indicated molar fraction x_{pip} of piperazine-based amide units. The indices of the crystalline reflections are indicated for the PA-2.14 homopolymer ($x_{pip} = 0$). The vertical offset of all graphs is proportional to x_{pip}. (a) 100 and 010/110 reflections, (b) 001 reflection, and (c) Lorentz-corrected diffraction intensity due to lamellar stacking. The dotted lines describe the general trend of the different peak positions and serve as a guide to the eye.

Results and Discussion

Examples of the X-ray diffraction patterns collected on the two homopolymers PA-2.14 and PA-pip.14, and a series of PA-(2.14-*co*-pip.14) copolymers with a varying molar fraction of piperazine-based units are shown in Figure 2. Three different Q ranges are displayed: (a) At high Q values between 1.3 and 1.7 Å^{-1}, two strong crystalline reflections can be recognized. In the case of the PA-2.14 homopolymer, they have been identified as the 100 and 010/110 reflections before.[6,7] The position of the 010 reflection directly represents the reciprocal distance between two successive hydrogen-bonded sheets. On the other hand, the reciprocal position of the 100 reflection is equal to the projection of the interchain

distance within a hydrogen-bonded sheet on the normal of a 100 lattice plane. (b) At intermediate Q values around 0.35 $Å^{-1}$, the 001 reflections of the different samples are found. These represent the long repetition period connected with the rather long size of the fully stretched comonomers. The 001 planes are parallel to the surface of the lamella-shaped crystallites so that the 001 lattice spacing is equivalent to a projection of the comonomer length to the normal of the surface of the crystalline lamella. (c) The small Q regime between 0.03 and 0.1 $Å^{-1}$ presents the reflections associated with the repeat distance in the stacklike arrangement of crystalline lamellae.

In the high Q range (see Figure 2a), the diffraction pattern of PA-2.14 ($x_{pip} = 0$) is comparable to earlier results by Jones et al.[6] and Li and Yan.[7] As typical for 2.2*n* polyamides, the crystalline peaks corresponding to the 100 and 010/110 reflections are found to be less separated than in the case of most other even−even polyamides.[6,7] The second homopolymer PA-pip.14 ($x_{pip} = 1$) shows a diffraction pattern quite distinct from that of PA-2.14. Again, the wide-angle scattering is dominated by two crystalline reflections, but their position is clearly different from that of the 100 and 010/110 reflections of PA-2.14. The crystalline structure of PA-pip.14 has not been determined yet, and an indexation of the peaks in the WAXS patterns can therefore not be given. The diffraction patterns of the copolymers resemble either that of pure PA-2.14 in the case of lower piperazine fractions or that of pure PA-pip.14 at higher molar fractions. The patterns for coPA 0.70 and 0.82 present peaks that stem from both types of crystalline structures, the PA-2.14-like and the PA-pip.14-like. This indicates that the two structures coexist in the studied copolyamides over the corresponding composition range. Outside this region of coexistence, the peak positions corresponding to the reflections from PA-2.14 and PA-pip.14 structures in the copolymers are visible depending on the molar fraction x_{pip}. Thereby, the position of the dominant reflection of the copolymers is shifted with respect to the corresponding reflection in the two homopolymers PA-2.14 and PA-pip.14, even for low amounts of incorporated comonomer. This implies that the crystalline structure is modified as soon as low mole percentages of piperazine groups are present in PA-2.14 macromolecules. In the same way, the incorporation of minor amounts of 1,2-EDA residues in PA-pip.14 changes the crystal structure of pure PA-pip.14. Hence, the piperazine groups are in fact incorporated in the crystalline structure of the copolyamides and are not expelled into the amorphous fraction as it would be the case for noncocrystallizable comonomers. Also, the observation that a coexistence of two different crystalline structures is observed only in a rather small concentration range leads to the same conclusion; i.e., the EDA-based and piperazine-based amide units do indeed crystallize into a common crystalline structure. The similarity of the copolymer diffraction patterns to either one or the other of the two homopolymers patterns suggests that the general features of the corresponding crystalline structures are not severely affected by the introduction of piperazine-based units to PA-2.14 or EDA-based units to PA-pip.14 below a critical concentration of incorporated units. Thus, the PA-(2.14-*co*-pip.14) copolyamides can be expected to show the same structure of stacked, hydrogen-bonded sheets as it is the case for PA-2.14 over a composition range of $x_{pip} = 0-0.62$ and partially also in the coPA 0.70 and 0.82 samples.

The PA-2.14-like structure in the copolyamides is maintained up to relatively high concentrations of piperazine before it switches to the PA-pip.14 structure. A similar behavior, namely the crossover from one type of crystalline structure in a cocrystallizing polymer system to another as a function of the comonomer concentration, was found for random poly(ethylene terephthalate-*co*-ethylene naphthalene-2,6-dicarboxylate) (PET/PEN) copolymers by Lu and Windle.[15] Nevertheless, the corresponding mechanisms that are responsible for this behavior are not the same for PET/PEN and PA-(2.14-*co*-pip.14) copolymers. In the case of PET/PEN systems, the dimensions of the two cocrystallizing chemical units are not comparable. To cocrystallize within a PEN environment, the bonds of the smaller PET unit have to stretch in order to make it compatible with the PEN structure. This has been demonstrated by Wendling et al. via molecular dynamics simulations.[16] Because of this effect, the PET units adapt more easily to PEN environments than vice versa. Consequently, a rather high number of PET units can be incorporated (up to about 70 mol %) before the crystalline structure of PET/PEN copolymers is crossing over from the PEN type to the PET type.

In the copolyamides studied here, structural distortions of the two different chemical units upon cocrystallization can be neglected due to their very similar spatial extensions. The reasons for the preferred formation of the PA-2.14-like structure in the copolyamides appear to be directly related to the hierarchy of different binding forces within the polyamide material and their relative importance. The crystalline structure of polyamides is determined by three different binding mechanisms. First, the atoms of the polymer chains are connected via covalent forces. Second, hydrogen bonds are formed between the carboxyl and amine residues of neighbored parts of polyamide molecules. In this way, the polyamide chains are organized in two-dimensional, hydrogen-bonded sheets of folded chains. Third, van der Waals forces between the hydrogen-bonded sheets are responsible for the assembly of these sheets into stacks.[5] Since hydrogen bonds in general are stronger than dipolar or van der Waals interactions, they are playing here a dominant role in the crystallization. In the present example, this is demonstrated by the fact that the PA-2.14-like structure, which consists of stacked hydrogen-bonded sheets, can still be observed at a rather high molar fraction of piperazine of up to $x_{pip} = 0.82$. Although the density of hydrogen bonds is already considerably reduced at such an elevated piperazine fraction, the strength of the hydrogen bonds is apparently still high enough to ensure, at least partially, the formation of the typical stacked sheet structure of polyamides.

The behavior of the 001 reflection of the copolyamide as a function of molar fraction x_{pip} is shown in Figure 2b. Only one single peak is observed over the full composition range. Because of the lack of a clear double peak structure in the diffractograms, no immediate conclusion concerning the coexistence of two crystalline phases in the copolymers is possible. Nevertheless, important shifts of the peak position are observed in the range where the coexistence of the PA-2.14-like and the PA-pip.14-like structure is documented in the WAXS patterns for molar fractions of $x_{pip} = 0.70$ and 0.82 (see

Figure 2a). Apparently, the crystalline order in the direction of the long *c* spacing, which is represented by the 001 reflection, is similar for both crystalline phases in the coexistence region. Such a behavior can be understood as a consequence of the chemical connectivity of the chain molecules. As the two types of residues within the copolymers are connected via covalent bonds, the crystalline order in the direction of the chain axis is predefined by the structure of the chemical repeat units. Now, if the individual crystalline phases are very small, they will be interconnected due to the fact that each polymer chain participates in many of these phases. This provides a strong constraint to both crystalline structures. We consider the formation of two individual unit cells differing only in the **a** and **b** axes and sharing a common **c** or chain axis to be the easiest way for the system to adapt to this condition. Expressed in a different way, this means that the tilt angle of the chains with respect to the lamella surface are the same for both coexisting crystalline phases. This also implies that the typical size of the PA-2.14- and PA-pip.14-like phases are small compared to the typical thickness of the crystalline lamellae. Outside the presumed coexistence range, the peak positions depend only weakly on x_{pip}, which corroborates the assumption of only one single crystalline phase, very similar to either the PA-2.14 or PA-pip.14 type being present in this case.

The SAXS patterns in Figure 2c show one single broad reflection from the lamellar stacks at all molar fractions of piperazine-based units. With increasing x_{pip}, the position of the lamellar reflection shifts to lower Q values corresponding to a larger average lamellar thickness. It is to be noted that all samples were subjected to the same thermal history. This trend corresponds well to the behavior that can be expected upon the incorporation of a chemical unit that increases the stiffness of the polymer chain. As is the case for the crystalline 001 reflection, it is not possible to distinguish two individual lamellar reflections. This corroborates that the size of the coexisting crystalline phases must be assumed to be much smaller than the repeat distance between two successive lamella (which is typically in the range of some hundreds of angstroms).

The lattice spacings d_{hkl} corresponding to the different crystalline peaks in the diffraction patterns were determined by a fit of a corresponding number of Lorentz functions plus an additional background term consisting of a broad Lorentzian and a linear background that accounted for the underlying amorphous halo. The lattice spacings were obtained from the fitted peak positions via the relation $d_{hkl} = 2\pi/Q_{hkl}$. In the case of the SAXS results on the periodic lamellar stacking, the scattered intensity was corrected with the appropriate Lorentz factor; i.e., the intensity data were multiplied by Q^2.

The lattice spacings d_{hkl} corresponding to the position of the diffraction peaks are shown in Figure 3 as a function of the piperazine molar fraction x_{pip}. The repeat distance d_{lam} of the lamellar stacking shows a steady, nearly linear increase with increasing piperazine molar fractions, starting at a value around 90 Å and reaching a maximum of about 120 Å. The lattice spacing d_{001} decreases steadily with increasing x_{pip} from the value of 19 Å for the PA-2.14 homopolymer to 16.5 Å for the PA-pip.14 homopolymer with increasing x_{pip}. It shows a moderate slope at lower piperazine molar fractions between 0.00 and 0.54, but the range between x_{pip} = 0.62 and 1.00 is marked by a much steeper slope. The latter interval corresponds roughly to the composition range where also the coexistence of crystallites with PA-2.14 and PA-pip.14 structure is expected to occur. By a closer look on the d_{lam} and d_{001} data, systematic deviations between diffraction patterns taken immediately after the heating/cooling cycle (BM26B and ID11 measurements) and after several hours of annealing at room temperature (ID2 measurements) can be identified. This observation suggests a possibility, which strengthens further, that the crystalline structure in the recrystallized materials is still relaxing at room temperature during the annealing time. Furthermore, it demonstrates that these relaxations are only affecting the large-scale structure of the crystallites, as the deviations can only be observed in the large repeat distances d_{lam} and d_{001} but not in the shorter d_{100} and $d_{010/110}$ spacings (see Figure 3c,d). It is to be noted that in these polymers T_g varies between 60 and 50 °C with increasing piperazine content.

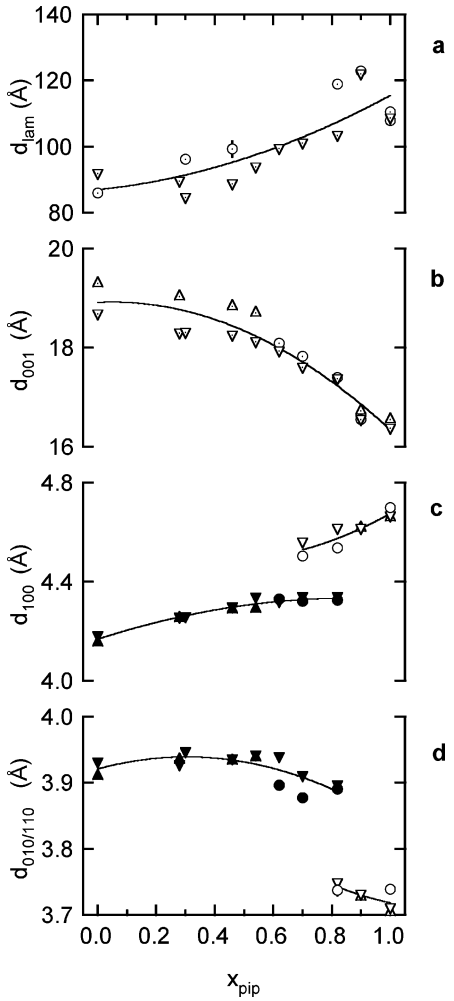

Figure 3. Lamellar and crystalline repeat distances of piperazine-based copolyamides over the molar fraction x_{pip}: (a) d_{lam}, (b) d_{001}, (c) d_{100}, and (d) $d_{010/110}$, from BM26B (circles), ID11 (up triangles), and ID2 (down triangles). Filled symbols: crystalline phase with PA-2.14-like structure; unfilled symbols: crystalline phase with PA-pip.14 structure; unfilled symbols with dot: no differentiation between different crystalline phases. All lines serve as a guide to the eye.

As the two different crystalline structures in the coexistence range can be distinguished due to their distinct diffraction patterns, it is possible to analyze phases with PA-2.14 and PA-pip.14-like crystalline

structures separately. Although the detailed crystalline structure of PA-pip.14 is still unknown and hence no crystalline indices for the PA-pip.14 reflections can be assigned at the moment, the corresponding repeat distances for the PA-pip.14-like structure are shown together with the closest d_{hkl} value for the PA-2.14-like structure in Figure 3c,d. While the relative changes in the different lattice spacings of the PA-2.14 in the copolyamides over the molar fraction of piperazine are moderate and do not exceed a value of 5%, the lamellar repeat distance increases by 30−40% (see Figure 3a). This illustrates that the morphology of the polyamide crystallites, as characterized by the lamellar repeat distance, is much stronger affected by the incorporation of piperazine groups than the structure within the crystallites themselves.

The lattice spacing for the 001 planes in the crystalline structure, as experimentally determined from the diffraction patterns, can now be compared with the length of a chemical repeat unit of the polymer chain. This latter quantity corresponds to the length of the c axis of the crystallographic unit cell for the triclinic structure generally found for polyamides.[5] Assuming a fully stretched conformation of the PA-2.14 polymer chain, a value of $c = 22.3$ Å can be calculated from the typical bond lengths and angles of the covalent bonds that are forming the backbone of the polymer.[7] The distance between the two nitrogen atoms in 1,2-EDA and in piperazine is comparable, and consequently the build-in size of the two respective comonomers also becomes practically identical. Hence, the replacement of 1,2-EDA groups in PA-2.14 by piperazine units will hardly affect the repeat distance along the stretched polymer chain or, equivalently, the length of the crystallographic c axis. The lattice spacing d_{001} is related to the length of the (real space) lattice vector **c** by the relation

$$d_{001} = c \cos \vartheta_c \tag{1}$$

where ϑ_c denotes the angle between the crystallographic c-axis and the normal of the 001 lattice plane represented by the reciprocal lattice vector $\mathbf{r}_c$. As the direction of the c-axis coincides with the chain axis of the polymer and as the normal on the 001 planes is identical to the normal on the corresponding crystalline lamella, the angle ϑ_c is identical to the tilt angle of the polymer chains with respect to the normal of the lamella surface.

The values of the tilt angle ϑ_c that were obtained from eq 1 are presented in Figure 4. Three different regimes can be identified in the dependence of the tilt angle ϑ_c on the molar fraction of piperazine-based units. A moderate linear trend dominates over a wide composition range including the pure 1,2-EDA-based polyamide and stretching out to molar fractions of up to 0.62. In a similar way, the concentration dependence of ϑ_c is relatively weak for samples with a high piperazine content of $x_{pip} = 0.90-1.00$. Compared to this, the tilt angle varies more strongly between $x_{pip} = 0.62$ and 0.90. The x_{pip} interval showing the increased concentration dependence of ϑ_c corresponds again to the region where the coexistence of PA-2.14- and PA-pip.14-like structures was observed in the WAXS patterns. When the crystalline structure is allowed to relax before the X-ray diffraction measurements, the tilt angles ϑ_c are shifted toward higher values compared to nonrelaxed structures. This effect is stronger for samples where the piperazine-based units are the minority component than

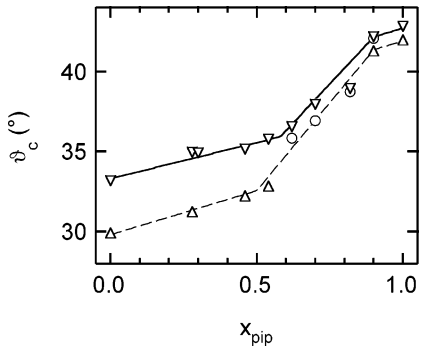

Figure 4. Tilt angle ϑ_c of the copolyamide chain axis with respect to the lamella normal over the molar fraction x_{pip} of piperazine-based amide units as determined from BM26B (circles), ID11 (up triangles), and ID2 (down triangles) measurements. The lines serve as a guide to the eye: continuous line, after relaxation at room temperature; dashed line, immediately after recrystallization.

for samples that are rich in piperazine. This observation agrees with the idea that the incorporation of piperazine groups will increase the mobility of the copolymer molecules within the crystalline structure because of the reduced number of hydrogen bonds. Therefore, the crystalline structure in piperazine-rich materials will be closer to equilibrium right after the recrystallization procedure than in the case of samples with low piperazine content. This implies a smaller margin for relaxations during annealing at room temperatures for materials with a higher piperazine molar fraction.

While the results presented above illustrate how the tilt angle of the polymer chain varies with the increasing piperazine content in polyamide copolymers, it remains to be clarified to which structural changes of the crystallites they correspond. This question is treated in the following paragraphs. For a complete description of a triclinic crystalline structure it is necessary to determine the six lattice parameters a, b, c, α, β, and γ. These lattice parameters are related to the reciprocal lattice vectors $\mathbf{r}_a$, $\mathbf{r}_b$, and $\mathbf{r}_c$ by the equations

$$\mathbf{r}_a = \frac{\mathbf{b} \times \mathbf{c}}{V_c} \tag{2}$$

$$\mathbf{r}_b = \frac{\mathbf{c} \times \mathbf{a}}{V_c} \tag{3}$$

$$\mathbf{r}_c = \frac{\mathbf{a} \times \mathbf{b}}{V_c} \tag{4}$$

where $V_c = \mathbf{a}\cdot(\mathbf{b} \times \mathbf{c})$ is the volume of the crystalline unit cell.[17] The lattice spacings d_{hkl} of PA-2.14 considered here are identical to the reciprocal length of the corresponding reciprocal lattice vector: $d_{100} = 1/r_a$, $d_{010} = 1/r_b$, and $d_{001} = 1/r_c$. In the present case, there are only three experimental quantities available but six unknowns to be determined. To overcome this lack of experimental information, three assumptions concerning the crystalline structure of the studied polyamide copolymers are made: (i) The length of the unit cell vector **c** is considered to be identical to the distance from one chemical building unit to the next along the polymer chain for all copolymers that show the presence of a PA-2.14-like structure in the recrystallized material. This is justified due to the very similar length of the 1,2-EDA and the piperazine units. The value for c is

assumed to be independent of the relative amount of piperazine in the copolymer, and the value found for the PA-2.14 homopolymer is applied for all copolymers showing the PA-2.14-like crystalline structure.

The inter- and intrachain interactions are dominated by the hydrogen bonds between the polyamide chains. Their predominance over other interactions between the molecules is corroborated by the fact that the PA-2.14-like structure, which is based on hydrogen-bonded sheet substructures, is the only structure found for molar fractions over a wide copolymer composition range from $x_{pip} = 0.00$ to 0.62 and is still present up to $x_{pip} = 0.82$. At the same time the PA-pip.14-like structure, which is not based on hydrogen bonds, can be found in a relatively small interval from $x_{pip} = 0.70$ to 1.00, only. Consequently, the incorporation of the piperazine units into the PA-2.14-like structure affects mainly the lattice parameters that are controlled by interactions weaker than hydrogen bonding. On the basis of these considerations, two further assumptions concerning the PA-2.14 structure in the copolymers are justified: (ii) The hydrogen bonds should remain perpendicular with respect to the backbone of the polyamide chains, and (iii) the length of the hydrogen bonds, and hence the interchain distance within the plane of a sheet, is assumed to be independent of the concentration of piperazine units. These assumptions express that the crystalline structure within the hydrogen-bonded sheets should hardly depend on the molar fraction of piperazine-based units for the PA-2.14-like structures found in the copolyamides studied here. In terms of lattice parameters, this means that the three parameters a, c, and β, which describe the structure within the hydrogen-bonded sheets, can be considered as practically independent of the piperazine content. Therefore, literature values for these three lattice parameters corresponding to pure PA-2.14, i.e., $a = 4.90$ Å, $c = 22.3$ Å, and $\beta = 77°$,[7] were used for all PA-2.14-like structures found at different molar fractions. This approach represents the idea that the observed changes in the lattice spacings d_{hkl} upon the incorporation of piperazine can be fully explained by variations in the stacking of the hydrogen-bonded sheets alone while the intrasheet structure can be assumed to depend only weakly on the piperazine content. Hence, the observed variations in the peak positions of the different reflections (see Figures 2 and 3) can be attributed to a modification of the relative position of two successive hydrogen-bonded sheets rather than to changes within the sheet structure itself.

One important question is how the piperazine rings are actually built into the structure of the hydrogen-bonded sheets of the copolyamides. The interchain distance within the plane of these sheets is larger than it would be for the corresponding crystalline structure of polyethylene, where no hydrogen bonds are present. Effectively this means that the hydrogen bonds keep the chain backbones of the molecules that are involved in the bonding further apart from each other than in the case of comparable polymers without hydrogen bonds. In this situation, it appears plausible that the piperazine rings can be incorporated into the structure of a hydrogen-bonded polyamide sheet without any major modification of the in-plane interchain distance. In contrast to the interchain distance of the polymers within a sheet, the intersheet distance is not determined by hydrogen bonds, and a dense packing of successive sheets is realized in polyamide crystallites. The incorporation of piperazine rings with the plane of the rings standing perpendicular to the plane of the hydrogen-bonded sheets would immediatly increase the intersheet distance, which could be directly measured via the position of the 010 reflection. Our experimental results reveal practically no change of the intersheet distance with the molar fraction of incorporated piperazine groups over the full composition range, where the PA-2.14-like structure was observed. Hence, the piperazine rings within the PA-2.14-like structure of the copolyamides are coplanar with the hydrogen-bonded sheets. This conclusion is in full agreement with the sp^2-hybridization of a piperazine nitrogen incorporated into an amide functionality.

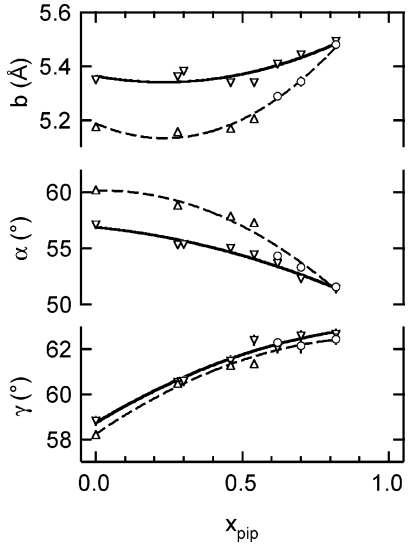

Figure 5. Lattice parameters b, α, and γ of copolyamides over the molar fraction x_{pip} of piperazine-based amide units for the crystalline phase showing PA-2.14 structure, determined from BM26B (circles), ID11 (up triangles), and ID2 (down triangles) measurements. The dotted lines serve as a guide to the eye.

The stacking of the hydrogen-bonded sheets is represented by the remaining lattice parameters b, α, and γ. They essentially describe the lateral rearrangement of the hydrogen-bonded sheets within the stack structure (here as a function of the piperazine content in the copolymer). These three quantities were determined by a best fit to the experimental d_{hkl} values of each copolymer with the further lattice parameters fixed to values given above. The results are shown in Figure 5. The displayed lattice parameters directly represent the distortion of the crystalline unit cell of the PA-2.14-like structure upon the incorporation of piperazine groups. It can be observed that the parameters found vary in a systematic manner. Up to a value of $x_{pip} = 0.54$, the parameter b shows hardly any concentration dependence. Beyond this limit it increases in a nearly linear fashion. The angles α and β show a nonlinear behavior over the full concentration range covered. While α decreases, γ increases with increasing x_{pip}. All relative changes in these three parameters are on the order of 10% for the highest observable piperazine concentrations.

The distortion of the crystalline unit cell upon the incorporation of piperazine groups into the polyamide structure is evident from Figure 5. A systematic difference between the results from relaxed (circles and up triangles) and nonrelaxed (down triangles) concerning the positioning of successive hydrogen-bonded sheets with respect to the direction of the c-axis can be

recognized. A possible explanation of the observation could be that upon cooling the materials the crystalline and amorphous parts of the lamellar stacks change their density at different rates. This creates internal tensions in the materials that act on the surface of the crystalline lamellae. The crystalline structure will rearrange under these external and directed forces on a given characteristic time scale. The experimental results show that the relaxation of the crystalline structure can be identified as a displacement of the hydrogen-bonded sheets parallel to the *c*-axis, which coincides with the axis of the polymer chains in the crystallites, rather than perpendicular to it. Annealing after the cooling cycle allows the copolymer to release the internal tensions by relaxations in the amorphous phase (provided that the annealing temperature is above the glass transition temperature of the polymer) and, as we conclude from our results, also by relaxation in the crystalline phase.

Conclusions

By applying XRD, the spacings of the 100, 010, and 001 lattice planes of PA-(2.14-*co*-pip.14) copolymers were determined from the corresponding reflections in the diffraction patterns. Two different crystalline structures were observed that resemble the two homopolymers PA-2.14 and PA-pip.14. The structural changes of the PA-2.14-like crystalline structure in the copolyamides were evaluated assuming that the typical stacked-sheet organization of the crystalline structure of polyamides is maintained and that the geometry of the hydrogen bonds is practically not affected by the incorporation of piperazine groups. From the fact that the intersheet distance in the polyamide crystallites does not depend on the molar fraction of piperazine-based comonomers, it is concluded that the piperazine groups are oriented parallel (or close to parallel) to the hydrogen-bonded sheets. In the given framework, the concentration dependence of the experimentally determined lattice spacings is explained as the result of a modification in the stacking of the hydrogen-bonded sheets alone, while the intrasheet structure is essentially preserved. This finding is in good agreement with the intuitive picture of strongly bonded sheet substructures in polyamides.

Acknowledgment. The authors express their gratitude to the Netherlands Organisation for Scientific Research and to the European Synchrotron Radiation Facility for providing beamtime on the respective experimental devices, to the Dutch Polymer Institute and the Eindhoven University of Technology for financial support of the project, and to M. Basiura, I .P. Dolbnya, D. Detollenaere, G. Heunen, and J. Jacobs for their support during the X-ray diffraction experiments.

References and Notes

(1) Brydson, J. A. *Plastic Materials*, 7th ed.; Butterworth-Heinemann: Oxford, UK, 1999; Chapter 18.
(2) Evstatiev, M. In *Handbook of Thermoplastics*; Olabisi, O., Ed.; Marcel Dekker: New York, 1997; Chapter 27.
(3) Jones, N. A.; Atkins, E. D. T.; Hill, M. J. *J. Polym. Sci., Part B: Polym. Phys.* **2000**, *38*, 1209.
(4) Vanhaecht, B.; Devroede, J.; Willem, R.; Biesemans, M.; Goonewardena, W.; Rastogi, S.; Hoffmann, S.; Klein, P. G.; Koning, C. E. *J. Polym. Sci., Part A: Polym. Chem.* **2003**, *41*, 2082.
(5) *Nylon Plastics Handbook*; Kohan, M. I., Ed.; Carl Hanser Verlag: Munich, Germany, 1995.
(6) Jones, N. A.; Cooper, S. J.; Atkins, E. D. T.; Hill, M. J.; Franco, L. *J. Polym. Sci., Part B: Polym. Phys.* **1997**, *35*, 675.
(7) Li, W.; Yan, D. *Cryst. Growth Des.* **2003**, *3*, 531.
(8) Jones, N. A.; Atkins, E. D. T.; Hill, M. J.; Cooper, S. J.; Franco, L. *Macromolecules* **1996**, *29*, 6011.
(9) Jones, N. A.; Atkins, E. D. T.; Hill, M. J.; Cooper, S. J.; Franco, L. *Polymer* **1997**, *38*, 2689.
(10) Jones, N. A.; Atkins, E. D. T.; Hill, M. J.; Cooper, S. J.; Franco, L. *Macromolecules* **1997**, *30*, 3569.
(11) Ramesh, C. *Macromolecules* **1999**, *32*, 3721.
(12) Kvick, Å. *Nucl. Instrum. Methods Phys. Res. B* **2003**, *199*, 531.
(13) Bras, W.; Dolbnya, I. P.; Detollenaere, D.; van Tol, R.; Malfois, M.; Greaves, G. N.; Ryan, A. J.; Heeley, E. *J. Appl. Crystallogr.* **2003**, *36*, 791.
(14) Urban, V.; Panine, P.; Ponchut, C.; Boesecke, P.; Narayanan, T. *J. Appl. Crystallogr.* **2003**, *36*, 809.
(15) Lu, X.; Windle, A. H. *Polymer* **1995**, *36*, 451.
(16) Wendling, J.; Gusev, A. A.; Suter, U. W. *Macromolecules* **1998**, *31*, 2509.
(17) Guinier, A. *X-Ray Diffraction in Crystals, Imperfect Crystals, and Amorphous Bodies*; Dover Publications: New York, 1994.

MA048456E